Published in final edited form as:
*Bioorg Med Chem*. 2014 February 15; 22(4): 1362–1369. doi:10.1016/j.bmc.2013.12.064.

# Insights into the Mechanism of Streptonigrin-Induced Protein Arginine Deiminase Inactivation

**Christina J. Dreyton**[1], **Erin D. Anderson**[2], **Venkataraman Subramanian**[1], **Dale L. Boger**[2], and **Paul R. Thompson**[1,*]

[1]Department of Chemistry and The Kellogg School of Graduate Studies, The Scripps Research Institute-Florida, 130 Scripps Way, Jupiter, FL 33458

[2]Department of Chemistry and The Skaggs Institute for Chemical Biology, The Scripps Research Institute, 10550 North Torrey Pines Road, La Jolla, CA 92037

## Abstract

Protein citrullination is just one of more than 200 known PTMs. This modification, catalyzed by the Protein Arginine Deiminases (PADs 1–4 and PAD6 in humans), converts the positively charged guanidinium group of an arginine residue into a neutral ureido-group. Given the strong links between dysregulated PAD activity and human disease, we initiated a program to develop PAD inhibitors as potential therapeutics for these and other diseases in which the PADs are thought to play a role. Streptonigrin which possesses both anti-tumor and anti-bacterial activity was later identified as a highly potent PAD4 inhibitor. In an effort to understand why streptonigrin is such a potent and selective PAD4 inhibitor, we explored its structure-activity relationships by examining the inhibitory effects of several analogues that mimic the A, B, C, and/or D rings of streptonigrin. We report the identification of the 7-amino-quinoline-5,8-dione core of streptonigrin as a highly potent pharmacophore that acts as a pan-PAD inhibitor.

### Keywords

PADs; Streptonigrin; 7-amino-quinoline-5,8-dione; Protein arginine deiminase; Irreversible inhibitors

## 1. Introduction

Post-translational modifications (PTMs) are an added layer of regulation that finely tune the physiological functions of the cell. Protein citrullination is just one of more than 200 known PTMs. This modification, catalyzed by the Protein Arginine Deiminases (PADs 1–4 and PAD6 in humans), converts the positively charged guanidinium group of an arginine residue into a neutral ureido-group.[1] As a consequence, this PTM can enhance or inhibit protein-protein interactions, and potentially disrupt protein-DNA and protein-RNA interactions. For example, citrullination of Arg2142 in the GRIP1 binding domain of p300 prevents the



*Corresponding author. Tel.: +1-561-228-2860; fax: +1-561-228-2918; pthompso@scripps.edu.

Supplementary Material
Figures S1–S3, and Table S1 including detailed figure legends.

methylation of the same arginine residue by co-activator associated arginine methyltransferase 1 (CARM1), which consequently disrupts the interaction between p300 and GRIP1, a nuclear receptor co-activator.[2] As a consequence, this modification leads to decreased expression of genes under the control of the estrogen receptor.[2]

With the potentially wide ranging effects of this PTM, it is unsurprising that several diseases (e.g., multiple sclerosis, rheumatoid arthritis (RA), and Colitis), are associated with aberrantly increased PAD activity.[1] For example, the deterioration of the myelin sheath in multiple sclerosis correlates with the hyperdeimination of myelin basic protein.[3] Since PAD2 is the predominant PAD in the brain, dysregulated PAD2 activity has been suggested to play a principle role in the onset and progression of this disease.[3,4] In addition, one of the most well studied links between dysregulated PAD activity and human disease is the one that exists with RA. For example, the presence of a PAD4 mutation correlates with an increased risk of developing RA in Asian populations;[5] these mutations are thought to increase PAD4 mRNA stability leading to the overexpression of PAD4.[5] PAD2 also likely plays a role because both it and PAD4 are overexpressed in the synovial joints of these patients.[6] Importantly, aberrant citrullination is associated with the development of anti-citrulline protein antibodies whose presence is highly diagnostic and predictive of RA.[7,8]

Given the strong links between dysregulated PAD activity and human disease, we initiated a program to develop PAD inhibitors as potential therapeutics for these and other diseases in which the PADs are thought to play a role. From our initial efforts, we identified Cl-amidine as an irreversible pan-PAD inhibitor[9] and used it to show that the PADs play an important role in gene transcription and NET formation.[10–15] For example, Cl-amidine was used to show that PAD2 activity is important for the high level of expression of estrogen receptor-α target genes via its ability to citrullinate histone H3 at R26.[13] Additionally, Cl-amidine, or an analog, decrease disease severity in animal models of RA, spinal cord injury, ulcerative colitis, lupus and cancer, thereby helping to validate the PADs as therapeutic targets.[16–21] 2-chloroacetamidine, the reactive portion of Cl-amidine, was also recently shown to decrease disease severity in several animal models of multiple sclerosis.[22]

Although Cl-amidine has proven to be an extremely useful tool compound, it shows only modest selectivity between the PAD isozymes, and it is therefore difficult to use this compound to ascribe a particular function to a specific PAD. To identify PAD inhibitors with improved selectivity, we developed a Fluorescence-Polarization-Activity-based Protein Profiling (FluoPol-ABPP) based high-throughput screen to identify novel PAD inhibitors and chemotypes that could be further derivatized to generate highly potent and selective inhibitors.[23] From an initial validation screen, we identified streptonigrin (Figure 1) as a potent and selective irreversible PAD4 inhibitor; streptonigrin preferentially inhibits PAD4 by 119-, 37-, and 126-fold versus PADs 1–3, respectively.[23]

Streptonigrin, a natural product produced by *Streptomyces flocculus*, possesses both anti-tumor and anti-bacterial activity. In eukaryotic cells, cytotoxicity is thought to primarily stem from effects on DNA stability, as this compound has been shown to induce strand breaks in a transition metal and NADH-dependent manner.[24–26] Streptonigrin also inhibits topoisomerase II, which enhances the DNA damaging effects of this compound [27]. The ability of streptonigrin to induce the formation of reactive oxygen species may also contribute to cell death.[24] Given the fact that streptonigrin is a highly potent PAD4 inhibitor, the anti-neoplastic effects of this compound may also be due in part to its ability to inhibit PAD4.[23]

In an effort to understand why streptonigrin is such a potent and selective PAD4 inhibitor, we explored its structure-activity relationships by examining the inhibitory effects of several

key partial structures that mimic the A, B, C, and/or D rings of streptonigrin (see Figure 1 for ring naming nomenclature). Herein, we report the results of these studies. Specifically, we show that the quinoline-5,8-dione portion of streptonigrin (A and B rings) is required for enzyme inactivation, that the pyridyl C ring and its substituents can significantly impact potency, and that rings C and D are likely required for isozyme selectivity. We also identified several derivatives from these efforts and report here that 7-amino-quinoline-5,8-diones are highly potent pan-PAD inhibitors(**Compounds 3, 14, and 21**) both *in vitro* and in cells.

## 2. Results and Discussion

### 2.1. Library Screening

Structurally, streptonigrin consists of four rings designated A, B, C, and D that correspond to the quinoline-5,8-dione (Ring A and B), the central pyridine (Ring C), and the substituted phenyl ring (Ring D). To determine the contributions of these components to the potency and selectivity of streptonigrin, we screeneda small, focused 32 member compound library that structurally mimics the A, B, C and D rings (Figure 2). For these studies, each member of the library (10 μM each) was tested against the active PAD isozymes, PADs 1, 2, 3, and 4 (PAD6 is not active) to obtain percent activity values (Table 1).[7]

Examining the structures of the most potent compounds, it is clear that the quinoline-5,8-dione portion is critical for the potency of streptonigrin, as analogues of the C and D rings (e.g., **compounds 4, 6,7, and 8**) showed little to no inhibition of the PADs. In contrast, the quinoline-5,8-dione moiety appears essential for potency as a number of analogs incorporating this functionality show strong inhibition of the PADs (e.g. **compounds 3, 10, 14, 17, and 21**). From this analysis, it is also clear that an oxidized quinoline-5,8-dione core is necessary for potent inhibition because napthoquinones (**compound 19**) show only modest inhibition (~50%) and non-oxidized quinolines (**compounds 29** and **30**), show no inhibition even when bound to pyridines (**compounds 5 and 23**), triazines (**compounds 25 and 26**) or more extended scaffolds (**compound 24**). Remarkably, removing the pyridyl nitrogen from the C ring led to loss in potency even with an analogue that contains the active 7-aminoquinoline-5,8-quinone (**compound 22**), indicating that ring C and its substituents can markedly influence potency.

Although the quinoline-5,8-dione core is essential for strong inhibition of the PADs (see data for **compounds 3, 10, 14, 17, and 21**), substitutions around the ring have a variety of effects on potency. For example, analogs in which the 6-methoxy group of the quinoline-5,8-dione is removed (**compound 14**) or replaced with a bromine (**compound 21**) either maintained or increased their potency for PADs 1–4.

Surprisingly, however, introduction of a bromine at the 6 or 7 positions on its own tempered the potency of several quinoline-5,8-diones (e.g., **compounds 2, 9, 16, and 20**) but this effect could be rescued by the introduction of an electron-donating group in combination with the bromine at either of these two positions (compare **compounds 10** and **21** to **compound 2**). While the reason for this effect is not known, it is likely related to changes in the reactivity of the quinoline-5,8-dione for enzyme inactivation.

Based on both the percent activity (Table 1) screens and $IC_{50}$ values (Supplementary Table 1), these studies identified analogues **1, 3, 10, 14, 17,** and **21** as the most potent inhibitors of PADs 1–4. With the exception of analogue **10**, the top hits all contain a 7-amino group. Further studies to prioritize these 7 compounds and characterize their mechanism(s) of inhibition are described below.

### 2.2. Reversibility Studies

Given that quinoline-5,8-diones are known Michael acceptors and that streptonigrin irreversibly inhibits PAD4, the structures of the top hits suggested that their activity could be derived from their ability to irreversibly inhibit the PADs.[23] To test this hypothesis, we treated PAD4 with an excess of compounds **3**, **10**, **14**, **17**, and **21** (100 μM) before dialysis to remove unbound inhibitor. These samples were then tested for the recovery of enzymatic activity (Figure 3A). The results indicate that little to no activity is recovered after dialysis confirming that these compounds are irreversible PAD4 inhibitors. To test whether this property was unique to PAD4, or shared amongst the other isozymes, we performed complementary experiments with PADs 1, 2, 3 and 4, focusing on **17,** the most potent analogue. For these experiments, each of the PADs was incubated with a 170-fold excess of **17**, and then dialyzed for 20 h (Figure 3B). Little to no activity was regained, thus confirming that these compounds irreversibly inhibit all of the active PAD isozymes. Note that the small amount of residual enzyme activity is most likely due to incomplete inactivation as the enzyme levels remained the same before and after dialysis.

### 2.3. Selectivity Studies

To evaluate the selectivity amongst the active PAD isozymes, we determined $k_{inact}/K_{I(app)}$ values(Table 2) for each of the top hits. Note that $k_{inact}/K_I$ is a better measure of isozyme selectivity than $IC_{50}$ because $k_{inact}/K_I$ is a second order rate constant whereas $IC_{50}$ values for irreversible inhibitors are a product of both reversible binding and time dependent irreversible inhibition. For **3**, which is one of the simplest and most potent streptonigrin analogues, we also determined $k_{inact}$, $K_I$, and $k_{inact}/K_I$ values for PADs 2 and 4. We focused on these two isozymes because they are the most relevant to human disease.[1,7] For PAD4, inactivation by **3** yielded $k_{inact}$, $K_I$, and $k_{inact}/K_I$ values of 0.12 ± 0.01 $min^{-1}$, 20.1 ± 5.4 μM, and 5,700 $M^{-1}min^{-1}$, respectively(Figure 4). For PAD2, the values are 0.07 ± 0.003 $min^{-1}$, 8.08 ± 1.7 μM, and 8,300 $M^{-1}$ $min^{-1}$, respectively. Note that the higher $k_{inact}/K_I$ values obtained for PAD2 may relate to its ability to promote aggregation of this isozyme (Figure S1) but not PAD4 (Figure 5). Apparent $k_{inact}/K_I$ values for the top hits mirrored the $IC_{50}$ values as there was a ≤3-fold change in $k_{inact}/K_{I(app)}$ values between the four different PAD isozymes (Table 2). In total, these data indicate that while highly potent, these analogues lack selectivity amongst the PADs.

### 2.4. Gel-Based Competitive ABPP Studies

To determine whether these analogues can prevent labeling of an active site residue, we used our previously described gel-based ABPP assay.[23,28] Briefly, the PAD-targeted ABPPs, RFA and RCA covalently modify an active site cysteine and compete with an inhibitor for binding to the active site. Compounds that show strong inhibition will show minimal labeling by RFA and RCA, whereas weak inhibitors exhibit strong labeling by either of these probes.[28,29] For these studies, the concentration of RFA was fixed at 10 μM and increasing amounts of streptonigrin, **3**, and **17** were added to compete for ABPP labeling.

Note we focused here on **3** and **17** because **3** is one of the simpler analogues of the A, B and C rings whereas **17** is one of the most potent hits. As expected, increasing streptonigrin concentrations decreased the labeling of PADs 2 and 4 by RFA (Figure 5 and Figure S1). Like the parent compound, **3** and **17** also prevent labeling of PADs 2 and 4 by RFA suggesting that the quinoline-5,8-dione core covalently modifies an active site residue or alternatively prevents the adoption of the catalytically competent state (Figure 5 and Figure S1).

### 2.5. Substrate Protection Studies

In addition to our competitive ABPP studies, we determined whether a PAD substrate, BAEE, can protect against the **3**-induced inactivation of PAD4, similarly to streptonigrin.[23] Typically substrate protection assays measure initial rates of activity using progress curves and varying concentrations of substrate; thus BAEE protection of the PAD active site from inactivation would result in faster initial rates of activity upon higher substrate concentrations. Surprisingly, little substrate protection was observed for the **3**-induced inactivation of PAD4 (Figure S2). This result suggests PAD inactivation occurs not solely through modification of the active site but also by additional mechanisms.

### 2.6. MALDI Mass Spectrometry Analysis

To further interrogate the mechanism of streptonigrin inactivation, we examined the stoichiometry of inactivation by MADLI-MS. Upon treatment of recombinant WT-PAD4 with streptonigrin, **3**, and **17** in a 1:10 ratio (enzyme:inhibitor), the mass of PAD4 was shifted by 710, 692, and 945 Da, respectively (Figure 6 and Table 3). Similarly, sized mass shifts were also observed for PAD2; the mass of PAD2 was increased by 469, 324, and 853 Da, respectively (Figure S3). These mass shifts are significantly higher than what one would expect for a 1:1 enzyme:inhibitor complex suggesting that multiple sites on the enzyme are modified. To determine whether one of those sites corresponds to the active site, we also examined the stoichiometry of the PAD2C647A and PAD4C645A mutants which are catalytically inactive due to a Cys to Ala substitution of the active site nucleophile. Interestingly, the mass shifts of these catalytically inactive mutants are also significantly higher than expected for a 1:1 stoichiometry and are consistent with multiple covalent modifications (Figure 6). Note that super oxide dismutase and catalase had no effect on enzyme inactivation (not shown), suggesting the >1:1 stoichiometry is not due to these compounds promoting enzyme oxidation. In total these results, coupled with our ABPP and substrate protection studies, suggest that streptonigrin, **3** and **17** inactivate the PADs through multiple covalent modifications both within and outside of the active sites of these enzymes.

### 2.7. Cell Proliferation Studies

When first discovered, streptonigrin was heralded for its antibiotic activity and efficacy as an anti-cancer agent. So much so, that the compound was almost immediately put into clinical trials, however, it became quite clear that the high toxicity and side effects of the compound outweighed its benefits as an anti-cancer agent.[30] The mechanism(s) behind the cytotoxic nature of streptonigrin likely include DNA strand scission, Topoisomerase II-mediated DNA cleavage, the formation of DNA-damaging reactive oxygen species (ROS), and possibly PAD inhibition.[23,24,27,31,32] To determine if our keyanalogues possess selective anti-proliferative activities that might show greater efficacy in PAD-associated cancers, we assessed their biological activities by measuring cell viability in U2OS cells, an osteosarcoma cell line that overexpresses PAD4 and NIH 3T3 cells, a mouse embryonic fibroblast cell line.[11] At 10 μM, compound **3**, **14** and **21** are most effective in killing both U2OS and NIH 3T3 cells with ≤30% of cells remaining viable. $EC_{50}$ values for these compounds show that they possess a similar level of potency against U2OS and NIH 3T3 cells with ≤ 5-fold change in $EC_{50}$ values amongst analogues (Figure 7 and Table 4). In comparison, **10** and **17** are moderately effective as both cells lines retain significant viability at 10 μM (Figure 7) and the $EC_{50}$ value for **17** is 58.3 ± 8.7 μM in U20S cell(Figure 7 and Table 4). This phenomenon is also present in NIH 3T3 cells as cell viability is comparable to the DMSO control and an $EC_{50}$ value of 61 ±10.1μM. The reduced potency of **17** may be due to a reduction in its bioavailability due to the presence of a negatively charged carboxylate.

## 3. Conclusion

In conclusion, we developed a structure-activity relationship for streptonigrin that has provided unique insights into the streptonigrin-induced inactivation of the PADs. Specifically, we identified the quinoline-5,8-dione core, in particular, the 7-amino-quinoline-5,8-dione scaffold, as critical for PAD inhibition. The lead compounds (**3, 10, 14, 17, and 21**) exhibit $k_{inact}/K_I$ values that are comparable to our first and second generation mechanism-based inactivators, Cl-amidine[9] and Thr-Asp-F-amidine (TDFA)[33] whose $k_{inact}/K_I$ values are 13,000 and 26,000 $M^{-1}min^{-1}$, respectively. Additional studies comparing the second order rate constants of inactivation (i.e., $k_{inact}/K_I$) indicate that the inter-isozyme selectivity is ≤5-fold. Thus, while these compounds lack selectivity, their high potency could allow these scaffolds to serve as pan-PAD inhibitors.

Although it remains unclear how streptonigrin inhibits the PADs, the fact that quinoline-5,8-dione scaffold contains Michael acceptors suggest that inhibition is due to the covalent modification of the enzyme, which was confirmed by MALDI-MS. Since the stoichiometry of modification by compounds **3** and **17** is >1, these data suggests a greater level of promiscuity associated with these streptonigrin analogues by contrast to its parent compound. We speculate that additional sites of modification may include other reactive non-disulfide bonded cysteines orlysine residues.

Finally, the cellular proliferation studies demonstrate that **3**, **14**, and **21** show a high degree of cytotoxicity towards both cancerous U2OS and normal NIH 3T3 cell lines. These results suggest cytotoxic properties associated with these analogues in addition to their ability to inhibit the PADs. In total, we have identified the quinoline-5,8-dione core as a potent PAD pharmacophore.

## 4. Experimental

### 4.1. Chemicals

Dithiothreitol (DTT), 4-(2-hydroxyethyl)-1-piperazineethanesulfonic acid (HEPES), ammonium iron (III) sulfate dodecahydrate, tris (2-carboxyethyl) phosphine (TCEP), and thiosemicarbazide were acquired from Sigma-Aldrich. Diacetyl monooxime (DAMO), N-α-Benzoyl-L-arginine ethyl ester (BAEE), and N-α-Benzoyl-L-arginine amide (BAA) were obtained from Acros. PADs 1–4 were purified analogously to previously described methods.[33,34]

### 4.2. Synthesis of Streptonigrin Analogues

Analogues (**1**, **2**, **10**, **13**, **14**,**17** and **21**) were prepared as previously disclosed or were available (**3–9, 11, 12, 15, 16, 18–20, 22–30**) from prior studies.[35–4435–4041–44] Analogues **31** and **32** were prepared from analogue **2** as described below:

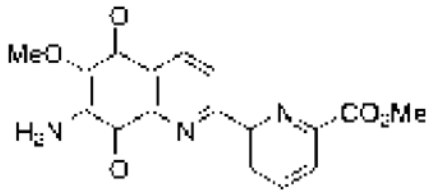


$CeCl_3$ (12.0 mg, 0.049 mmol, 1.0 equiv) and NaOMe (25% in MeOH, 22 μL, 0.097 mmol, 2.0 equiv) were added sequentially to a stirred solution of methyl 7-bromo-5,7-dioxo-2-(2′-pyridyl)quinoline-6′-carboxylate (**2**, 18.2 mg, 0.049 mmol) in MeOH (0.7 mL). After 30 min, the reaction mixture was filtered through Celite and concentrated on a rotary

evaporator. The resulting product was found to be sensitive to column chromatography and was used without further purification.

Sodium azide (6.9 mg, 0.11 mmol, 1.5 equiv) was added to a stirred solution of the crude 7-bromo-2-(6′-methoxycarbonyl-2′-pyridyl)-6-methoxy-quinoline-5,8-dione (28.7 mg, 0.07 mmol) in MeOH (2.5 mL) and DMF (2.5 mL) under Ar at RT in the dark. After 20 h, the reaction mixture was diluted with $H_2O$ (20 mL), and extracted with $CH_2Cl_2$ (5 × 15 mL). The combined organic extracts were washed with $H_2O$ (20 mL), dried ($Na_2SO_4$), and concentrated on a rotary evaporator. The crude azide was found to be sensitive to purification and was used without further purification.

10% Pd/C (5.4 mg) was added to a stirring suspension of the crude 7-azido-2-(6′-methoxycarbonyl-2′-pyridyl)-6-methoxy-quinoline-5,8-dione in EtOAc (5 mL) and EtOH (15 mL) under an $H_2$ atmosphere in the dark at RT. The reaction mixture was then stirred at RT under Ar for 18 h. After 18 h, the reaction mixture was filtered through Celite. Flash chromatography ($SiO_2$, EtOAc) provided 7-amino-2-(6′-methoxycarbonyl-2′-pyridyl)-6-methoxy-quinoline-5,8-dione (**31**) as a bright red solid (3.2 mg, 17%, over 3 steps):[451]H NMR ($CDCl_3$, 400 MHz) δ 8.88 (d, *J* = 8.4 Hz, 1H), 8.84 (d, *J* = 8.0 Hz, 1H), 8.51 (d, *J* = 8.0 Hz, 1H), 8.20 (d, *J* = 7.6 Hz, 1H), 8.01 (t, *J* = 8.0 Hz, 1H), 4.11 (s, 3H), 4.05 (s, 3H); ESI-TOF HRMS *m/z* 340.0924 ($[M + H]^+$, $C_{17}H_{13}N_3O_5 + H^+$ requires 340.0928).

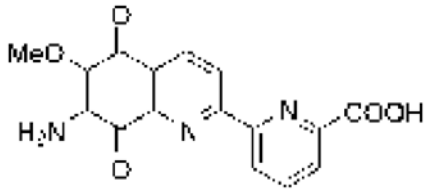


$Na_2S_2O_4$ (1.2 mg, 0.0069 mmol, 1.1 equiv) in H2O (0.1 mL) was added to a stirred solution of 7-amino-2-(6′-methoxycarbonyl-2′-pyridyl)-6-methoxy-quinoline-5.8-dione (**31**, 2.2 mg) in THF–$H_2O$ (0.7 mL, 1:1) under Ar at RT. After 30 min, KOH (1 M in $H_2O$, 53 μL, 0.053 mmol, 7.0 equiv) was added to the reaction mixture and stirring was continued at RT for 1 h. After 1 h, the reaction mixture was diluted with $H_2O$ (5 mL), acidified with addition of 10% aqueous HCl, and extracted with EtOAc (5 × 15 mL). The combined organic extracts were dried ($Na_2SO_4$) and concentrated on a rotary evaporator. Trituration of the crude residue with hexanes provided analogue **32** as an orange solid: $^1$H NMR (DMSO, 400 MHz) δ 8.84 (d, *J* = 8.0 Hz, 1H), 8.68 (d, *J* = 7.5 Hz, 1H), 8.45 (d, *J* = 8.5 Hz, 1H), 8.23 (t, *J* = 7.0 Hz, 1H), 8.18 (t, *J* = 8.0 Hz, 1H), 3.83 (s, 3H); ESI-TOF HRMS *m/z* 326.0778 ($[M + H]^+$, $C_{16}H_{11}N_3O_5 + H^+$ requires 326.0771).

### 4.3. Percent Inhibition Studies

The percent inhibition values for the streptonigrin analogues were determined in duplicateby incubating each compound (10 μM final) with recombinant wild-type PADs 1 and PAD4 (0.2 μM final) or PADs 2 and 3 (0.5 μM final) for 15 min in Reaction Buffer (10 mM $CaCl_2$, 2 mM DTT, 50 mM NaCl, and 100 mM Tris-HCl, pH 7.6 ). BAEE (10 mM final) was then added to initiate the reaction. After 15 min, the reaction was quenched and citrulline production was measured with the COLDER assay using previously described methods.[46,47]

### 4.4. $IC_{50}$ Values

$IC_{50}$ values were determined by incubating recombinant wild-type PADs 1 and 4 (0.2 μM final) or PADs 2 and 3 (0.5 μM final) with various concentrations of inhibitor for 15 min. BAEE (10 mM final) was then added and the reaction was allowed to proceed for 15 min

before quenching with liquid $N_2$. The experiments were completed in duplicate. $IC_{50}$ values were determined by fitting an eight-point dilution curve to equation 1,

$$\text{Fractional Activity} = 1/(1+[\text{I}]/\text{IC}_{50}) \quad (1)$$

using GraFit version 5.0.11.[48] $IC_{50}$ is defined as the concentration of inhibitor that provides 50% activity while [I] is the concentration of inhibitor.

### 4.5. Irreversibility Studies

Recombinant wild-type PAD4 and PAD2 (0.6 μM final) were incubated with streptonigrin, streptonigrin analogues, or no compound in Reaction Buffer (300 μL total reaction volume) for 1 h followed by dialysis into 2 L of Long-Term Storage Buffer (20 mM Tris-HCl, pH 7.6, 1 mM EDTA, 500 mM NaCl, 2 mM DTT, and 10% glycerol) for 20 h. Residual activity was measured as described above. Untreated controls for each of the isozymes were dialyzed separately and their percent activity remaining was set to 100%.

### 4.6. Gel-Based Competitive ABPP Studies

Recombinant wild-type PAD4 and PAD2 (2 μM final) were labeled with RFA (10 μM final) in the presence of calcium (10 mM final) and various concentrations of streptonigrin, **3** and **17** (0–50 μM final). Reactions were carried out in 50 mM HEPES, pH 7.6, 2 mM DTT, 50 mM NaCl for 1 h at 37 °C. 6X SDS-PAGE loading buffer (2.5 μL) was then added to each sample (20 μL final volume) to quench the reaction. The samples were boiled for 20 min and then the proteins were separated on a 12% SDS-PAGE gel. The relative fluorescence was visualized using a Typhoon imager and quantified with ImageQuant TL.

### 4.7. Streptonigrin Analogue Inactivation Studies

Inactivation reactions (100 mM Tris-HCl, pH 7.6, 10 mM $CaCl_2$, and 2 mM DTT) were incubated with PAD isozymes (PADs 1 and 4 (2 μM final) or PADs 2 and 3 (5.0 μM final) for 10 min at 37 °C in 60 μL total volume. An aliquot (6 μL) of this mixture was then immediately added to Reaction Buffer containing BAEE (10 mM final) to measure the residual activity at various time points (0–60 min). These reaction mixtures (60 μL total volume) were pre-incubated at 37 °C for 10 min before adding aliquots from the inactivation mixture. The final reaction proceeded for 15 min at which point the reaction was stopped by flash freezing in liquid $N_2$. Residual enzymatic activity was quantified using the methodology described above. The data obtained at each inactivator concentration were fit to equation 2,

$$v = v_0 e^{-kt} \quad (2)$$

using GraFit version 5.0.11. [48] where $v_o$ is the velocity, $v$ is the initial velocity, $k$ is the pseudo-first-order rate constant for inactivation, and $t$ is time. The $k_{inact}/K_{I(app)}$ values were determined by dividing the inactivation rate, $k_{obs}$, by the concentration of inhibitor.

### 4.8. Substrate Protection Studies

To evaluate the ability of substrate to protect against **3**-induced inactivation, progress curves were generated with and without inactivator (0.5 μM final) at two different concentrations of substrate. For **3**, BAEE concentrations of 2 mM ($2K_m$ for PAD4) and 10 mM ($5K_m$ for PAD4) were used. Reaction Buffer was pre-incubated for 10 min at 37 °C, and PAD4 (0.2 μM final) was added to initiate the reaction. Aliquots (60 μL) were taken at 0–8 min and data analysis was performed using equation 3,

$$\text{Product formation} = A_0\,(1 - e^{-kt})/k \quad (3)$$

where $A_0$ is the initial rate, $k$ is the pseudo-first order rate constant for inactivation, and $t$ is time.

### 4.9. MALDI Mass Spectrometry Analysis

Control and experimental reactions of PAD2 (3 μM final) and PAD4 (3 μM final) or their catalytically inactive mutants, PAD2 C647A (3 μM final) and PAD4 C645A (5 μM final) were incubated in a 1:10 ratio with streptonigrin or **3** in 100 mM HEPES, pH 7.6, 10 mM $CaCl_2$, and 2 mM DTT for 1 h. These reactions were dialyzed in $ddH_2O$ overnight, concentrated and eluted in sinapinic acid for analysis on a Microflex MALDI-TOF mass spectrometer (Bruker Daltonics).

### 4.10. XTT Assay

Mouse embryonic fibroblast NIH 3T3 and human osteosarcoma U2OS cell lines ($2.5 \times 10^4$ cells/mL) were treated with various concentrations of each streptonigrin analogue for 72 h in a 48 or 96-well plate. The 2,3-bis-(2-methoxy-4-nitro-5-sulfophenyl)-2*H*-tetrazolium-5-carboxanilide (XTT reagent) and N-methyl dibenzopyrazine methyl sulfate (PMS) activated solution (American Type Culture Collection) was added (50 μL) and incubated 4 h for color formation. The orange-colored formazan containing solution was then measured at an absorbance of 475 nm using a spectrophotometer. $EC_{50}$ values for cell growth inhibition were determined by fitting an eight-point dose response curves to equation 4,

$$Y = (\text{Range}/(1 + ([I]/EC_{50})^s)) + \text{Background} \quad (4)$$

using GraFit 5.0.11[48] where *Range* is the uninhibited value minus the background, and is *s* the slope factor.

## Supplementary Material

Refer to Web version on PubMed Central for supplementary material.

## Acknowledgments

This work was supported by NIH grants GM079357 (P.R.T.),MH084512 (D.L.B.) and CA042056 (D.L.B.).

## References and notes

1. Jones JE, Causey CP, Knuckley B, Slack-Noyes JL, Thompson PR. Curr Opin Drug Discov Devel. 2009; 12:616.
2. Lee YH, Coonrod SA, Kraus WL, Jelinek MA, Stallcup MR. Proc Natl Acad Sci U S A. 2005; 102:3611. [PubMed: 15731352]
3. Moscarello MA, Mastronardi FG, Wood DD. Neurochem Res. 2006; 32:251. [PubMed: 17031564]
4. Moscarello MA, Pritzker L, Mastronardi FG, Wood DD. J Neurochem. 2002; 81:335. [PubMed: 12064481]
5. Suzuki A, Yamada R, Chang X, Tokuhiro S, Sawada T, Suzuki M, Nagasaki M, Nakayama-Hamada M, Kawaida R, Ono M, Ohtsuki M, Furukawa H, Yoshino S, Yukioka M, Tohma S, Matsubara T, Wakitani S, Teshima R, Nishioka Y, Sekine A, Iida A, Takahashi A, Tsunoda T, Nakamura Y, Yamamoto K. Nat Genet. 2003; 34:395. [PubMed: 12833157]

6. Foulquier C, Sebbag M, Clavel C, Chapuy-Regaud S, Al Badine R, Mechin MC, Vincent C, Nachat R, Yamada M, Takahara H, Simon M, Guerrin M, Serre G. Arthritis Rheum. 2007; 56:3541. [PubMed: 17968929]
7. Vossenaar ER, Zendman AJ, van Venrooij WJ, Pruijn GJ. Bioessays. 2003; 25:1106. [PubMed: 14579251]
8. Schellekens GA, de Jong BA, van den Hoogen FH, van de Putte LB, van Venrooij WJ. J Clin Invest. 1998; 101:273. [PubMed: 9421490]
9. Luo Y, Arita K, Bhatia M, Knuckley B, Lee YH, Stallcup MR, Sato M, Thompson PR. Biochemistry. 2006; 45:11727. [PubMed: 17002273]
10. Li P, Li M, Lindberg MR, Kennett MJ, Xiong N, Wang Y. J Exp Med. 2010; 207:1853. [PubMed: 20733033]
11. Li P, Yao H, Zhang Z, Li M, Luo Y, Thompson PR, Gilmour DS, Wang Y. Mol Cell Biol. 2008; 28:4745. [PubMed: 18505818]
12. Zhang X, Gamble MJ, Stadler S, Cherrington BD, Causey CP, Thompson PR, Roberson MS, Kraus WL, Coonrod SA. PLoS Genet. 2011; 7:e1002112. [PubMed: 21655091]
13. Zhang XS, Bolt M, Guertin MJ, Chen W, Zhang S, Cherrington BD, Slade DJ, Dreyton CJ, Subramanian V, Bicker KL, Thompson PR, Mancini MA, Lis JT, Coonrod SA. Proc Natl Acad Sci U S A. 2012; 109:13331. [PubMed: 22853951]
14. Yao H, Li P, Venters BJ, Zheng S, Thompson PR, Pugh BF, Wang Y. J Biol Chem. 2008; 283:20060. [PubMed: 18499678]
15. Wang Y, Li M, Stadler S, Correll S, Li P, Wang D, Hayama R, Leonelli L, Han H, Grigoryev SA, Allis CD, Coonrod SA. J Cell Biol. 2009; 184:205. [PubMed: 19153223]
16. Chumanevich AA, Causey CP, Knuckley BA, Jones JE, Poudyal D, Chumanevich AP, Davis T, Matesic LE, Thompson PR, Hofseth LJ. Am J Physiol Gastrointest Liver Physiol. 2011; 300:G929. [PubMed: 21415415]
17. Lange S, Gogel S, Leung KY, Vernay B, Nicholas AP, Causey CP, Thompson PR, Greene ND, Ferretti P. Dev Biol. 2011; 355:205. [PubMed: 21539830]
18. Wang Y, Li P, Wang S, Hu J, Chen XA, Wu J, Fisher M, Oshaben K, Zhao N, Gu Y, Wang D, Chen G. J Biol Chem. 2012; 287:25941. [PubMed: 22605338]
19. Willis VC, Gizinski AM, Banda NK, Causey CP, Knuckley B, Cordova KN, Luo Y, Levitt B, Glogowska M, Chandra P, Kulik L, Robinson WH, Arend WP, Thompson PR, Holers VM. J Immunol. 2011; 186:4396. [PubMed: 21346230]
20. Knight JS, Zhao W, Luo W, Subramanian V, O'Dell AA, Yalavarthi S, Hodgin JB, Eitzman DT, Thompson PR, Kaplan MJ. J Clin Invest. 2013 in press. 10.1172/JCI67390
21. McElwee JL, Mohanan S, Griffith OL, Breuer HC, Anguish LJ, Cherrington BD, Palmer AM, Howe LR, Subramanian V, Causey CP, Thompson PR, Gray JW, Coonrod SA. BMC Cancer. 2012; 12:500. [PubMed: 23110523]
22. Moscarello MA, Lei H, Mastronardi FG, Winer S, Tsui H, Li Z, Ackerley C, Zhang L, Raijmakers R, Wood DD. Dis Model Mech. 2013
23. Knuckley B, Jones JE, Bachovchin DA, Slack J, Causey CP, Brown SJ, Rosen H, Cravatt BF, Thompson PR. Chem Commun (Camb). 2010; 46:7175. [PubMed: 20740228]
24. Bolzan AD, Bianchi MS. Mutat Res. 2001; 488:25. [PubMed: 11223403]
25. Anderberg PI, Harding MM. Anticancer Drug Des. 2001; 16:143. [PubMed: 11962512]
26. Anderberg PI, Harding MM, Lay PA. J Inorg Biochem. 2004; 98:720. [PubMed: 15134917]
27. Yamashita Y, Kawada S, Fujii N, Nakano H. Cancer Res. 1990; 50:5841. [PubMed: 2168283]
28. Knuckley B, Luo Y, Thompson PR. Bioorg Med Chem. 2008; 16:739. [PubMed: 17964793]
29. Luo Y, Knuckley B, Bhatia M, Thompson PR. J Am Chem Soc. 2006; 128:14468. [PubMed: 17090024]
30. Oleson JJ, Calderella LA, Mjos KJ, Reith AR, Thie RS, Toplin I. Antibiot Chemother. 1961; 11:158.
31. Testoni MI, Bianchi MS, Bianchi NO. In Vitro Cell Dev Biol Anim. 1993; 29A:623. [PubMed: 8376311]
32. Bolzan AD, Bianchi MS. Environ Mol Mutagen. 2004; 44:277. [PubMed: 15472926]

33. Jones JE, Slack JL, Fang P, Zhang X, Subramanian V, Causey CP, Coonrod SA, Guo M, Thompson PR. ACS Chem Biol. 2012; 7:160. [PubMed: 22004374]
34. Knuckley B, Causey CP, Jones JE, Bhatia M, Dreyton CJ, Osborne TC, Takahara H, Thompson PR. Biochemistry. 2010; 49:4852. [PubMed: 20469888]
35. Boger DL, Yasuda M, Mitscher LA, Drake SD, Kitos PA, Thompson SC. J Med Chem. 1987; 30:1918. [PubMed: 3656364]
36. Boger DL, Duff SR, Panek JS, Yasuda M. J Org Chem. 1985; 50:5782.
37. Boger DL, Panek JS, Duff SR. J Am Chem Soc. 1985; 107:5745.
38. Boger DL, Yasuda M. Heterocycles. 1986; 24:1067.
39. Boger DL, Panek JS. J Org Chem. 1983; 48:621.
40. Boger DL, Brotherton CE, Panek JS, Yohannes D. J Org Chem. 1984; 49:4056.
41. Boger DL, Panek JS, Duff SR, Yasuda M. J Org Chem. 1985; 50:5790.
42. Boger DL, Panek JS. Tetrahedron Lett. 1984; 25:3175.
43. Boger DL, Panek JS. J Org Chem. 1982; 47:3763.
44. Boger DL, Panek JS. Tetrahedron Lett. 1983; 24:4511.
45. Kimber M, Anderberg PI, Harding MM. Tetrahedron. 2000; 56:3575.
46. Kearney PL, Bhatia M, Jones NG, Luo Y, Glascock MC, Catchings KL, Yamada M, Thompson PR. Biochemistry. 2005; 44:10570. [PubMed: 16060666]
47. Knuckley B, Bhatia M, Thompson PR. Biochemistry. 2007; 46:6578. [PubMed: 17497940]
48. Leatherbarrow, RJ. Erathicus Software; Staines, UK: 2004.

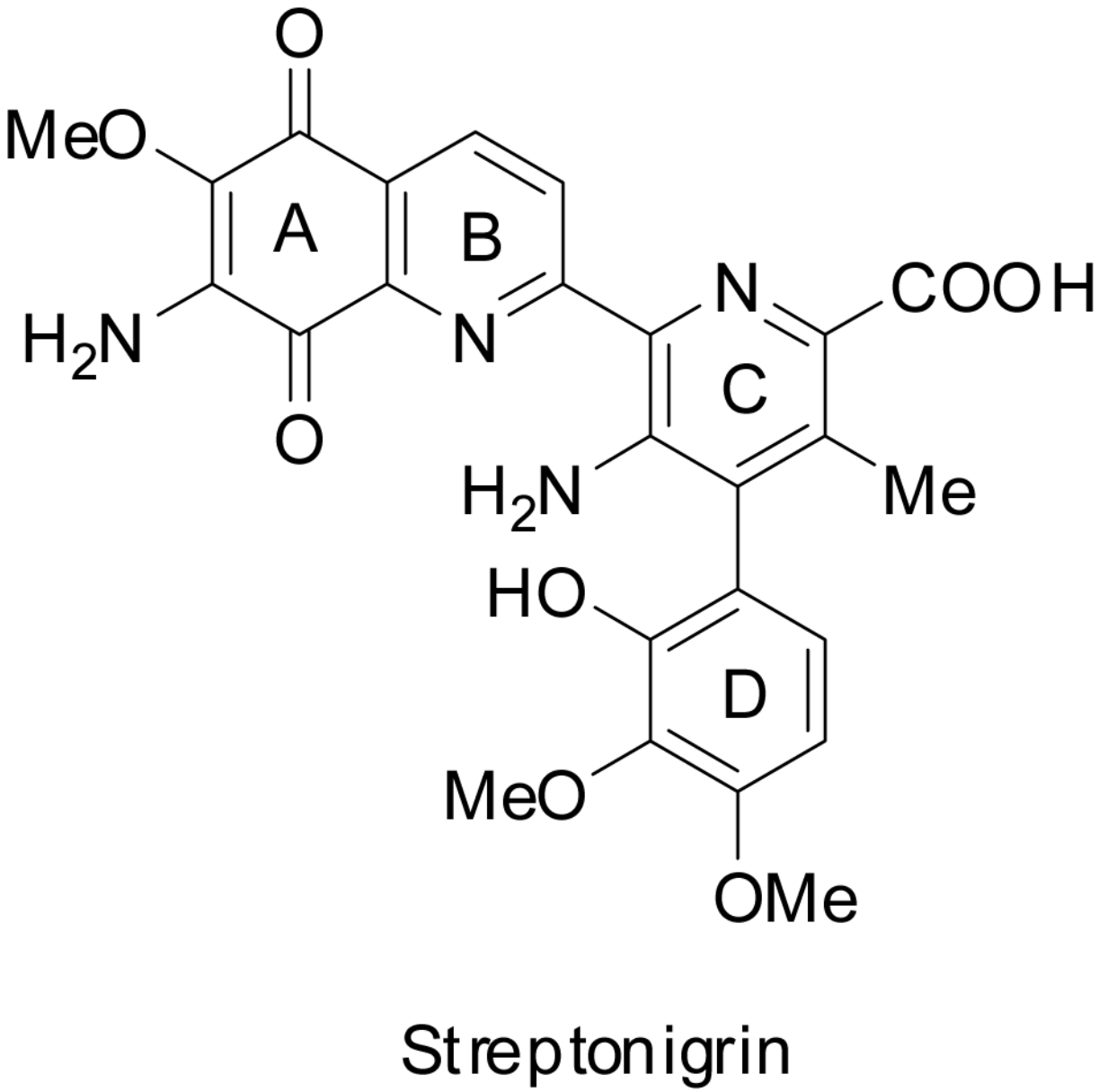


**Figure 1. Structure of Streptonigrin**

Streptonigrin is composed of four rings assigned A, B, C, and D. The fused A and B rings contain the quinoline-5,8-dione while the C and D rings contain the central pyridine and substituted phenyl portions of streptonigrin. Rings A, B, and C are co-planar while the D ring is perpendicular with respect to these rings.

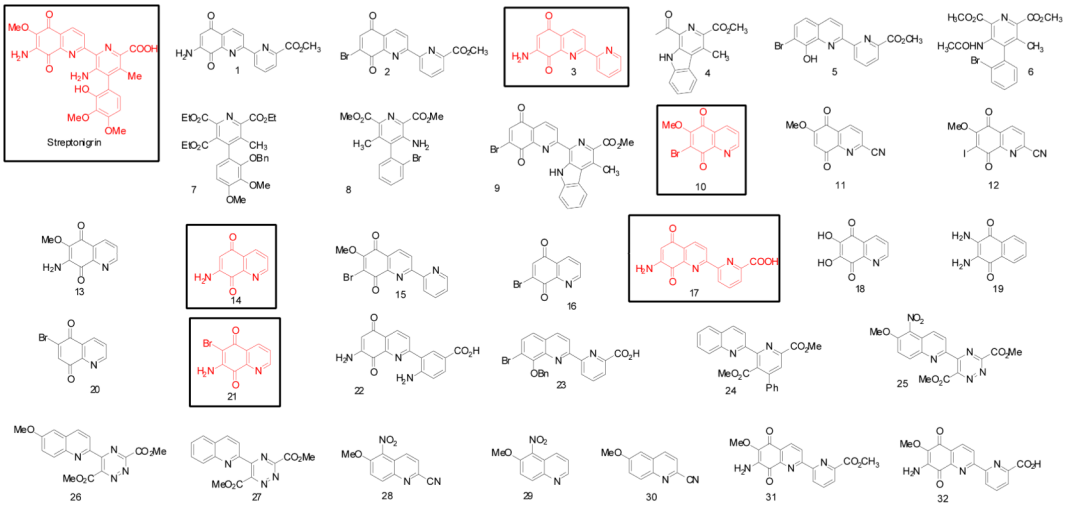


**Figure 2. Streptonigrin Compound Library**

The library is composed of 32 analogues of Streptonigrin. Streptonigrin and the most potent analogues are shown in red. Analogues **31** and **32** are the O-methyl derivatives of **1** and **17**.

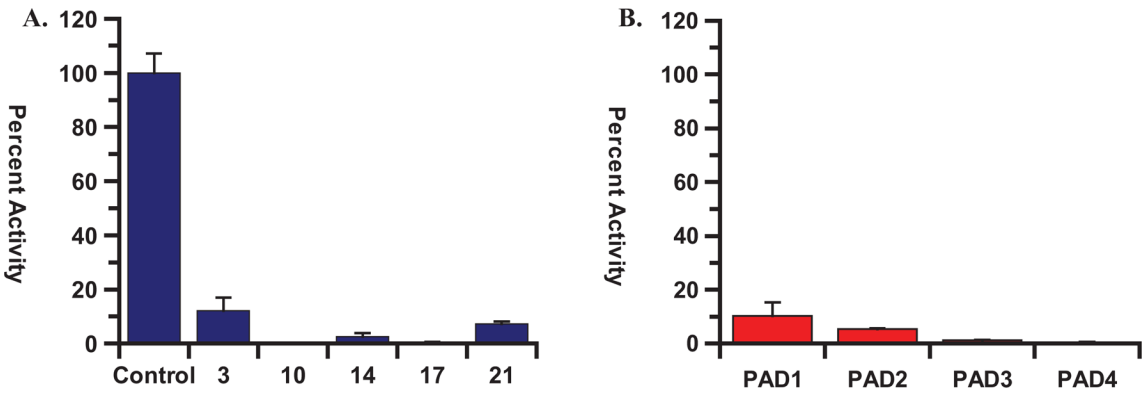


**Figure 3. Irreversibility Studies**

**(A)** Dialysis experiments demonstrate that the most potent streptonigrin analogues are irreversible PAD inhibitors. (**A**) Briefly, PAD4 (0.6 μM final) was incubated in Reaction Buffer with each analogue for 1 h. These reactions (300 μL final volume) were dialyzed overnight versus 2 L of Long-Term Storage Buffer. Percent activity was measured by incubating the 3-fold diluted reaction with 10 mM BAEE in Reaction Buffer for 10 min before quenching with liquid $N_2$. (**B**) The most potent analogue, compound 17 was used to demonstrate that it irreversibility inhibits all of the active PADs (PADs 1–4). Untreated controls for each of the isozymes were dialyzed separately and their percent activity remaining was set to 100%.

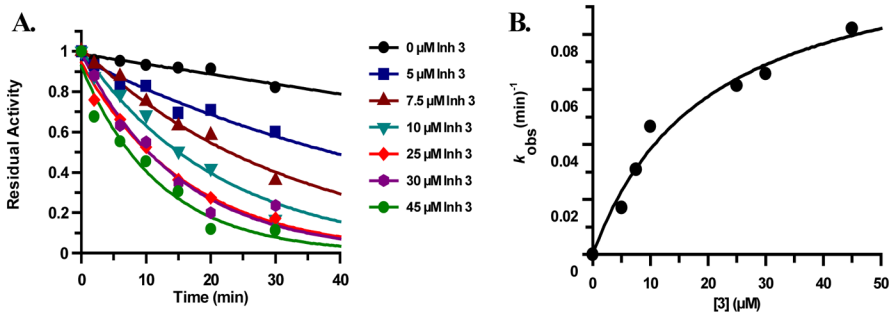


**Figure 4. Inactivation Kinetics of Analogue 3 with PAD4 and PAD2**

**(A)** Residual PAD4 activity was measured after incubation of **3** (0–45 μM) for 0–30 min. **(B)** Observed rates of inactivation, $k_{obs}$, for **3** and PAD4 were plotted against inhibitor concentration to determine values for $k_{inact}$, and $K_I$.

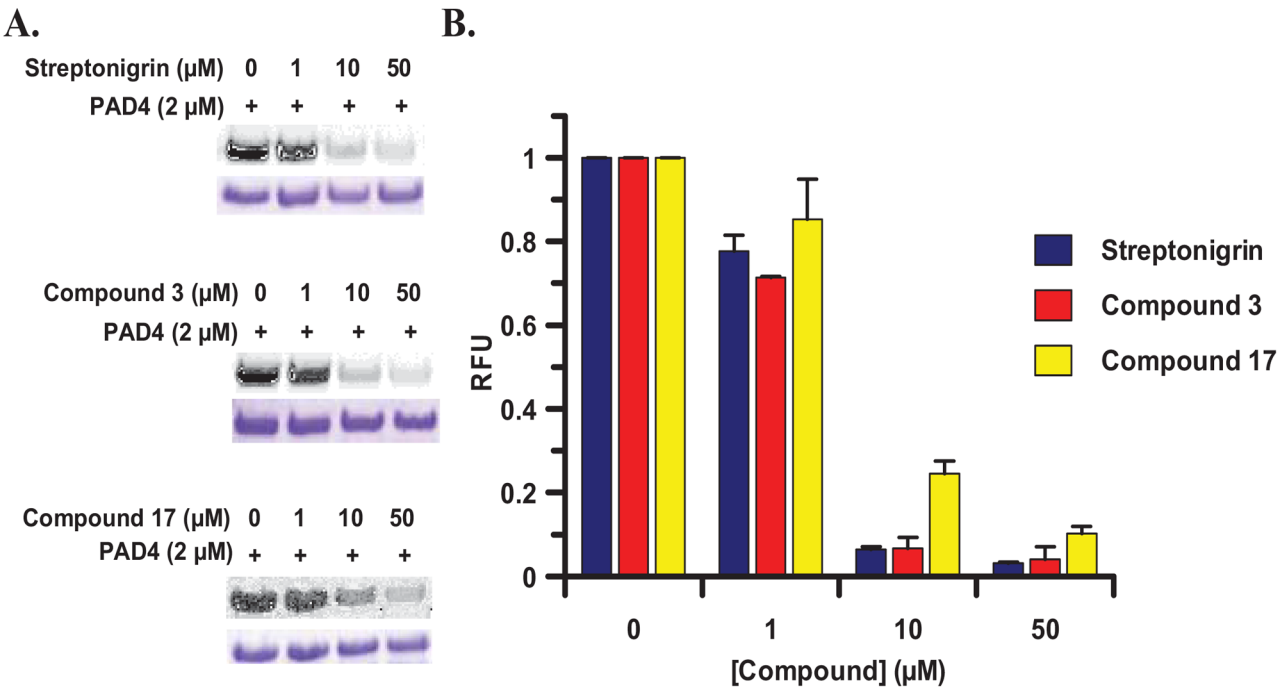


**Figure 5. Competitive ABPP Studies with Streptonigrin, 3, and 17**

Various concentrations of streptonigrin**, 3**, and **17** were competed with RFA for the labeling of 2 μM of wild-type PAD4.**(A)** In-gel fluorescence (top) and SDS-PAGE (bottom) of PAD4 by RFA in competition with 1, 10, and 50 μM, respectively of streptonigrin, **3**, and **17. (B)** Quantification of competitive ABPP assays with streptonigrin, **3**, and **17** for wild-type PAD4.

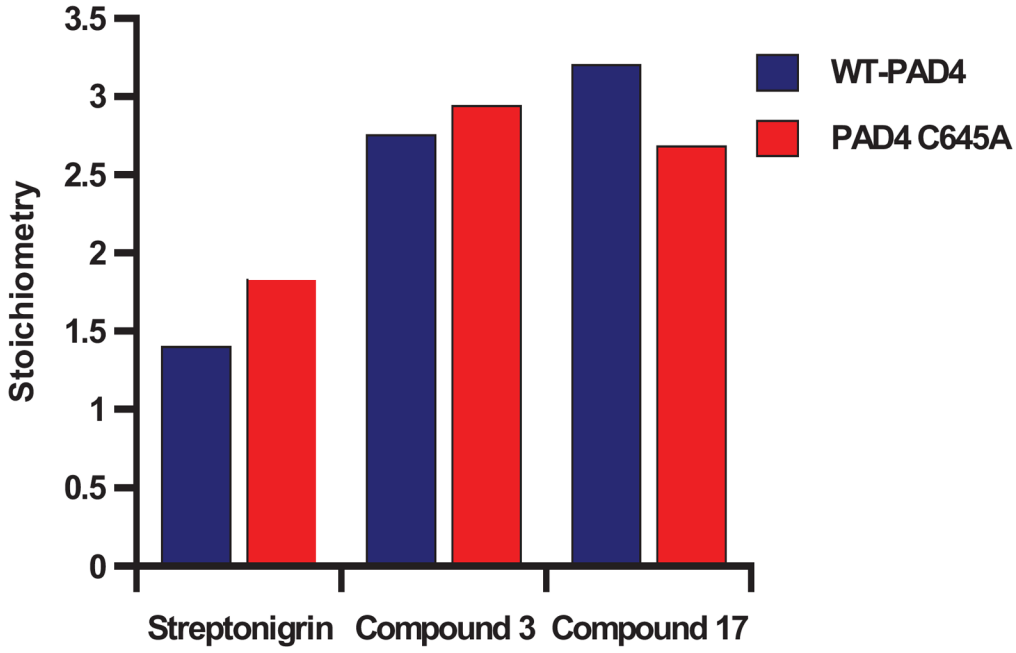


**Figure 6. MALDI-MS Analysis of PAD4 with Streptonigrin, Compound 3, and Compound 17**

**(A)** WT-PAD4 (3 μM) and PAD4C645A (5 μM) (catalytically inactive mutant) were reacted with streptonigrin, **3**, and **17** in a 1:10 ratio for 1 h before dialysis in $ddH_2O$. The recovered sample was concentrated by centrifugal evaporation and then analyzed by MALDI-MS.

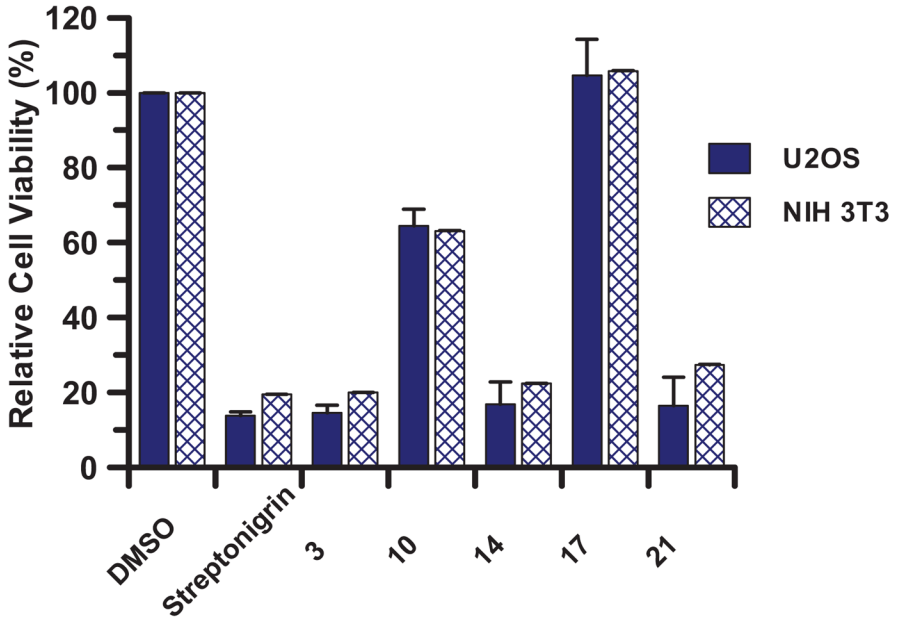


**Figure 7. XTT Assay of Streptonigrin and Top Hits**

XTT assays were performed with human osteosarcoma U2OS and mouse embryonic fibroblast NIH 3T3 ($2.5x10^4$ cells/mL) cell lines at 10 μM of streptonigrin, **3**, **10**, **14**, **17**, and **21**. Briefly, within 48-well plates (n=4)U2OS and NIH 3T3 cell were plated and dosed with 10 μM inhibitor for 3 days. After 3 days, the XTT-PMS (50 μL) reagent was added and allowed to incubate 4 h for color formation.

**Table 1**

Percent Activity at 10 μM Inhibitor.

| Inhibitor # | PAD1[a] | PAD2[a] | PAD3[a] | PAD4[a] |
|---|---|---|---|---|
| **1** | 24.5 ± 7.1 | 8.4 ± 1.8 | 16.4 ± 2.6 | 12.4±6.0 |
| **2** | 100.3 ± 6.6 | 126.4 ± 30.0 | 142.8 ± 30.2 | 75.7±2.3 |
| **3** | 26.9 ± 5.5 | 0 | 10.3 ± 0.4 | 15.3±2.6 |
| **4** | 95.3 ± 21.8 | 128.9 ± 9.2 | 119.8 ± 49.0 | 103.0±18.1 |
| **5** | 105.0 ± 14.1 | 122.5 ± 4.2 | 127.8 ± 3.3 | 100.2±11.6 |
| **6** | 119.8 ± 33.1 | 118.8 ± 0.8 | 130.4 ± 5.6 | 94.6±9.0 |
| **7** | 115.0 ± 6.3 | 131.0 ± 6.6 | 107.0 ± 22.6 | 101.7 ± 0.9 |
| **8** | 105.6 ± 17.6 | 122.4 ± 37.1 | 129.6 ± 20.9 | 99.8 ± 12.4 |
| **9** | 124.3 ± 54.9 | 115.2 ± 3.0 | 116.4 ± 19.2 | 100.8 ± 17.0 |
| **10** | 24.7 ± 13.6 | 11.8 ± 5.0 | 93.5 ± 7.07 | 10.1 ± 5.8 |
| **11** | 32.3±5.2 | 12.4 ± 32.0 | 0.89 ± 0.7 | 2.7 ± 4.5 |
| **12** | 39.8 ± 5.2 | 36.5 ± 34.6 | 1.7 ± 0.5 | 2.6 ± 2.7 |
| **13** | 43.2 ± 6.4 | 22.3 ± 3.3 | 0 | 12.7 ± 0.1 |
| **14** | 30.1 ± 7.4 | 10.9 ± 11.5 | 0.2 ± 2.7 | 1.0 ± 1.8 |
| **15** | 49.7 ± 11.7 | 38.3 ± 49.1 | 0.1 ± 0.5 | 9.5 ± 22.1 |
| **16** | 116.4 ± 13.6 | 86.5 ± 20.2 | 24.1 ± 16.1 | 43.7 ± 29.5 |
| **17** | 29.5 ± 5.1 | 14.9 ± 34.5 | 3.1 ± 1.4 | 1.6 ±1.2 |
| **18** | 61.2 ± 13.4 | 58.7 ± 25.6 | 4.0 ± 2.1 | 17.3 ± 28.2 |
| **19** | 78.1 ± 20.9 | 72.0 ± 7.6 | 56.0 ± 6.1 | 56.5 ± 39.7 |
| **20** | 156.7 ± 61.8 | 87.7 ±11.9 | 89.8 ± 34.3 | 90.0 ± 0.4 |
| **21** | 35.1±15.9 | 21.4 ± 10.6 | 4.8 ± 2.0 | 2.3 ± 0.5 |
| **22** | 113.0 ± 11.8 | 119.3 ± 7.1 | 91.5 ± 52.1 | 86.9 ± 23.1 |
| **23** | 122.6 ± 26.6 | 118.3 ± 13.2 | 106.9 ± 24.4 | 101.6 ± 44.8 |
| **24** | 120.3 ± 4.0 | 118.0 ± 13.2 | 83.8 ± 21.6 | 106.3 ± 9.4 |
| **25** | 138.0 ± 19.4 | 92.7 ± 2.6 | 82.0 ± 32.6 | 105.8 ±16.0 |
| **26** | 121.2 ± 24.7 | 113.6 ± 45.6 | 84.8 ± 24.4 | 96.9 ± 34.2 |
| **27** | 141.2 ± 32.5 | 113.2 ± 39.9 | 76.4 ± 19.0 | 107.7 ± 22.3 |
| **28** | 123.6 ± 16.7 | 97.9 ± 34.7 | 83.5 ± 55.6 | 97.8 ± 6.2 |
| **29** | 112.2 ± 13.2 | 82.6 ± 4.7 | 80.8 ± 36.6 | 107.5 ± 4.7 |
| **30** | 137.5 ± 43.5 | 64.8 ± 16.9 | 91.7 ± 40.7 | 110.4 ± 7.6 |
| **31** | 44.5 ± 0.6 | 52.9 ± 25.4 | 10.6 ± 5.0 | 40.5 ± 0.6 |
| **32** | 13.1 ± 15.9 | 29.9 ± 11.9 | 5.2 ± 1.2 | 9.1 ± 3.7 |

[a]Percent activity was determined by incubating recombinant wild-type PADs 1 and 4 (0.2 μM final) or PADs 2 and 3 (0.5 μM final) with 10 μM of inactivatior for 15 min. BAA (10 mM final: PAD1 and PAD3) or BAEE (10 mM final: PAD2 and PAD4) was then added and the reaction proceeded for 15 min before quenching with liquid $N_2$.

## Table 2

$k_{inact}/K_I$[a] Values for the Top Hits

| | $k_{inact}/K_I$ ($M^{-1}$ $min^{-1}$) | | | |
|---|---|---|---|---|
| **Compound** | **PAD1**[b] | **PAD2**[c] | **PAD3**[b] | **PAD4**[c] |
| **3** | 3200 | 8,300[d] | 1800 | 5700[d] |
| **10** | 3600 | 3800 | 1500 | 4900 |
| **14** | 4600 | 5200 | 3100 | 5600 |
| **17** | 3500 | 7300 | 1900 | 5300 |
| **21** | 4800 | 5000 | 1600 | 3500 |

[a] Inactivation reactions were incubated with recombinant wild-type PAD isozymes (PADs 1 and 4: 2 μM final or PADs 2 and 3: 5 μM final) for 10 min at 37 °C; 60 μL total volume). An aliquot of this mixture was then immediately added to Reaction Buffer containing BAEE or BAA (10 mM final) to measure the residual activity at various time points (0–30 min). The final reaction proceeded for 15 min at which point the reaction values were was stopped by flash freezing in liquid $N_2$. Apparent $k_{inact}/K_I$ calculated by dividing observed inactivation rate by the concentration of inhibitor.

[b] BAA used as a substrate.

[c] BAEE used as a substrate.

[d] Value is calculated from $k_{inact}$ and $K_I$.

## Table 3

MALDI-MS Analysis of Streptonigrin, Compound **3**, Compound **17**

| | Observed Da | | |
|---|---|---|---|
| | **Streptonigrin (506.5)** | **3 (251.2)** | **17 (295.2)** |
| **WT-PAD4** | 710 | 692 | 945 |
| **PAD4 C645A** | 924 | 737 | 792 |

Δ Da refers to the difference in Dalton of control versus inhibitor-treated experiments. The molecular weights of streptonigrin, 3, and 17 are shown in brackets below their names.

## Table 4

$EC_{50}$ (μM) Values of Analogues **3**, **14**, **17**, and **21**

| Compound | U2OS | NIH 3T3 |
|---|---|---|
| **3** | 0.4±0.01 | 0.6±0.04 |
| **14** | 0.8±0.04 | 1.1±0.2 |
| **17** | 58.3±8.7 | 61.7±10.6 |
| **21** | 1.6±0.08 | 0.4±0.05 |

$EC_{50}$ assays were performed with human osteosarcoma U2OS and mouse embryonic fibroblast NIH 3T3 cell lines at various concentrations **3**, **14**, **17**, and **21**. Briefly, within 96-well plates (n=8) cells ($2.5x10^4$ cell/mL) were plated and dosed with compound for 3 days. After 3 days, the XTT-PMS reagent (50 μL) was added and allowed to incubate 4 h for color development.